

# Seismic Performance Based Assessment of the Arsenal de Milly of the Medieval City of Rhodes

S. Cattari, A. Karatzetzou, S. Degli Abbatì, D. Pitilakis,  
C. Negulescu and K. Gkoktsi

**Abstract** The chapter focuses on the seismic performance based assessment (PBA) of the Arsenal de Milly, a 15th century masonry monument located in the Medieval City of Rhodes, in Greece. Although the structure is quite simple from a geometrical point of view, its seismic response is interesting due to the interaction effects with the massive adjacent defensive wall. In particular, the procedure proposed in the PERPETUATE project for the seismic protection of cultural heritage assets has been followed, by integrating the use of different modelling strategies to achieve a more reliable assessment and by exploiting also the use of ambient vibration tests for their calibration. The following modelling strategies have been adopted: (i) the finite element approach through a 3D model using brick finite elements (developed using the OpenSees code); (ii) the structural element modelling approach through a 3D model based on the equivalent frame approach (developed using the Tremuri software); (iii) the macro-block modelling based on the limit analysis according to the kinematic approach (developed using the MB-PERPETUATE software). The calibration of such models was supported by the results of ambient vibration tests, very

---

S. Cattari (✉) · S. Degli Abbatì  
Department of Civil, Chemical and Environmental Engineering,  
University of Genoa, Genoa, Italy  
e-mail: serena.cattari@unige.it

S. Degli Abbatì  
e-mail: stefania.degliabatti@unige.it

A. Karatzetzou · D. Pitilakis · K. Gkoktsi  
Department of Civil Engineering, University of Thessaloniki,  
Thessaloniki, Greece  
e-mail: akaratze@civil.auth.gr

D. Pitilakis  
e-mail: dpitilak@civil.auth.gr

K. Gkoktsi  
e-mail: kggkoktsi@gmail.com

C. Negulescu  
BRGM, Service DRP Avenue Claude Guillemin, 45060 Orleans, France  
e-mail: C.Negulescu@brgm.fr

useful in such case in order to highlight torsional modes related to the interaction effects with the massive adjacent defensive wall. Finally, some preliminary analyses on the soil—foundation—structure interaction effects have been included, too.

**Keywords** Historical masonry buildings · Seismic performance based assessment · Structural dynamic identification · FEM model · Equivalent frame model · Macro-block model

## 1 Introduction

This chapter focuses on the seismic performance-based assessment (PBA) of the Arsenal de Milly, an unreinforced masonry monument located in the Medieval City of Rhodes in Greece. In particular, the procedure proposed in the PERPETUATE project for performance-based earthquake protection of cultural heritage assets has been applied [19, 24].

The methodology developed in PERPETUATE adopts a displacement-based approach focused on the use of nonlinear analyses. A full methodological path for the assessment of cultural heritage assets has been proposed, which is based on three main steps. The first one includes: (1) classification of the architectonic asset and contained artistic assets; (2) definition of performance limit states and related safety and conservation requirements (specific for the cultural heritage assets); (3) evaluation of seismic hazard and soil-foundation interaction; (4) as built information (non-destructive testing, material parameters, structural identification) and definition of confidence factors by a sensitivity analysis on a preliminary model. The second step is related to: (5) finalization of structural models for the seismic analysis of the masonry building and the contained artistic assets (with identification of Performance Levels (PLs) on the pushover curves); (6) verification procedures. Finally, in the third step, rehabilitation decisions are taken and, if necessary, the second step is repeated for the design of strengthening interventions. In particular, the response variable assumed as the main outcome of PBA is the value of the Intensity Measure (IM) compatible with the fulfillment of performance levels (PL<sub>i</sub>) that have to be checked (IM<sub>PL<sub>i</sub></sub>): the proper IM has to be selected as a function of the features of the examined asset, while specific PLs have been proposed in PERPETUATE project with the aim of considering the safety and conservation in an integrated approach.

In this chapter, an application of such a procedure is presented focusing particular attention on substeps (4), (5) and (6) and briefly summarizing the results of the other substeps. Despite the apparent quite simple configuration of the examined structure, it represents the tool to deal with various interesting issues. In particular, the seismic response of the structure has been analyzed by comparing the results obtained from different modeling strategies, and in particular: (i) from the finite element approach (through a 3D model using brick finite elements); (ii) from structural element modeling (through a 3D model based on the equivalent frame

approach); (iii) from macro-block modeling. The option to integrate the use of such models in order to achieve a more reliable assessment is debated, discussing the limitations and advantages of each approach.

Moreover, results from microtremor measurements, carried out in step (4) and addressing the needs for structural identification of the building were useful in calibration of the mechanical parameters adopted in the models in the elastic range.

Finally, some preliminary results regarding the effects of soil-foundation interaction (SFI) have been illustrated, also.

## 2 Asset Classification and Performance Levels Considered

The first step (1) for the PBA is a proper interpretation of the seismic behavior expected for the given structure, which comes out from data collected about the as-built condition (Sect. 3).

Arsenal de Milly is located at the northeast corner of the medieval fortifications of Rhodes and it was built in the middle of the 15th century. It is a one storey rectangular building covered by a pointed vaulted ceiling, and characterized by the presence of a very thick and massive fortified wall which supported one of its sides (Fig. 1). This monument was subjected to many interventions in the past (as briefly illustrated in Sect. 3 and summarized in Fig. 3). Nowadays, it has been restored and the south wall is laterally supported by five buttresses (Figs. 2b).

In the PERPETUATE project a proper asset classification of the cultural heritage has been proposed [23] that is based on the prevailing seismic damage modes of assets and on the assumption that their occurrence is closely related to building morphology (architectural form, proportions) and technology (type of masonry, nature of horizontal diaphragms, and effectiveness of wall-to-wall and floor-to-wall connections). Such classification is then functional for the proper choice of the models to be adopted for seismic assessment [4].

The seismic response of the Arsenal de Milly is mainly affected: in the transversal direction, by the arch system realized by the vault; in the longitudinal one, by the in-plane response of masonry walls. The presence—as a unique diaphragm

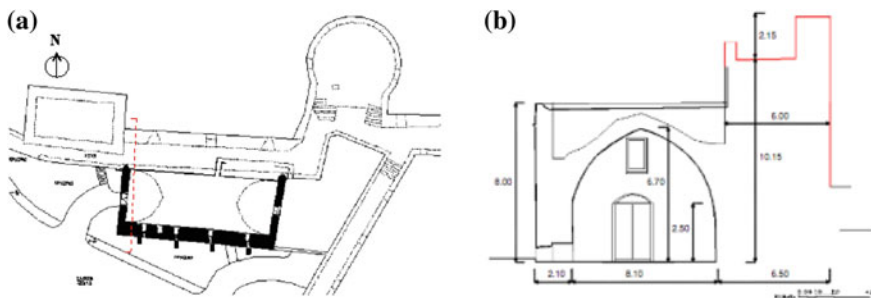
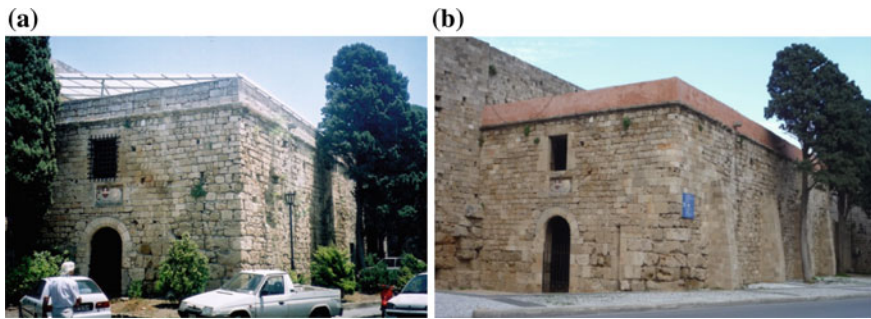


Fig. 1 Ground plan (a) and cross-section (b) after the restoration



**Fig. 2** The Arsenal de Milly before (a) and after (b) the restoration [25, 31]

aimed to couple the masonry walls—of the vault characterized by a limited stiffness would suggest the possibility to reasonably analyze such types of response also independently. However, the presence of the massive fortified wall highlights the need to investigate the possible interaction effect through a global model.

According to these issues and with reference to the architectural asset classification above mentioned, Arsenal de Milly belongs to Class B—*Assets analyzable by independent macroelements*, which are subjected to damage classes D (arch structures loaded in their vertical plane) and A (in plane damage of vertical walls). The vulnerability of the asset to damage class D has been also proven by past events (Fig. 4) as discussed in the next section, even if partially mitigated by the recent strengthening interventions. Indeed, such type of seismic response is very important for the examined case, due to its specific features (e.g. due to the presence of the buttresses and the high thickness of walls) as taken into consideration in the studied models.

Once the asset has been classified, step (2) requires the definition of the performance levels and related safety and conservation requirements, that is the definition of the *objectives* of the PBA for the examined asset.

According to the procedure illustrated in [19], PERPETUATE guidelines consider various performance levels identified by the alphanumeric code  $kn$ , where  $k = 1, 4$  is the level of performance and  $n = U, B, A$  is related to three different categories of requirements: *use and human life* (U), *building conservation* (B) and *artistic assets conservation* (A).

For each selected PL the related earthquake hazard levels, expressed in terms of return period ( $\bar{T}_{kn}$ ), have to be defined by eventually applying the importance coefficients  $\gamma_n$  ( $n = U, B, A$ ) to the basic values of the target return periods assumed for the given  $k$ -th PL (equal to 72, 100, 475 and 2475 years, respectively for  $k$  varying from 1 to 4). The importance coefficients may assume values greater or less than one, depending on the building relevance and conditions of use (e.g. unused, used for public or private functions, etc.).

In the case of Arsenal de Milly (since the building is not used for public functions and not relevant artistic assets are present) the seismic assessment has been checked only with regard to the 3B—*Significant but restorable damage* performance level; moreover, assuming  $\gamma_B = 1$ , the  $\bar{T}_{3B}$  value assumed corresponds to 475 years.

### 3 As Built Information

In this sub-step, geometrical, technological and mechanical features of the asset have been analyzed in depth. Several data have been acquired related to: geometry of the building; foundations; mechanical parameters; historical data on transformation and damage; state of maintenance; dynamic behavior. Indeed, as briefly summarized in Fig. 3, Arsenal De Milly has been subjected to many interventions in the past before arriving in its current configuration (phase e).

From a geometrical point of view, it is a building of rectangular plan and average dimensions of 10.20 m  $\times$  23.88 m (Fig. 1). It is covered by a vaulted ceiling. The vault has not the usual semi-cylindrical shape, but it is pointed at an average height of 6.70 m. It consists of the original (bearing) arch at a height of 2.50 m at its genesis and a thickness 0.25 m and has an overlying layer of mortar (kourasani) and an additional (non-bearing) thin “skin” of masonry ( $t = 0.25$  m), while in the past it had been filled with a layer of clay material. The support for the vault is achieved monolithically at the south (outer) side with the 2.10 m thick outer wall and at the northern tip (internal) is jointed and supported by a massive residual part of the ancient Wall of the Medieval Fortifications (having a thickness of 6.00 m).

The south wall and the vault, as well as the fortification wall, are made of ashlar masonry. The structure is founded at  $-1.90$  m below the ground; it consists of ashlar masonry, being a natural extension of the vertical walls of the structure with no widening. In situ and laboratory tests concerning the shape and the depth of foundation, via exploratory sections gave as a result the differential settlement observed in the direction perpendicular to the longitudinal axis of the Arsenal, perhaps because of soft soil profile combined with the different rigidity of each wall. Such evidence suggested also a possible significant contribution of SFI effects as discussed in more detail in Sect. 5.4.

Its damage pattern, before the restoration, highlights the vulnerability of the asset to out-of-plane response. Cracks of width up to 8 cm at the vertical walls and declinations at the top up to 10 cm led to partial detachment of both vault and south wall (Fig. 4). As aforementioned, nowadays, it has been restored and the south wall is laterally supported by five buttresses (Fig. 2b). These latter are made of ashlar masonry and are founded on a continuous footing and connected with the south wall both at the foundation and the superstructure.

In the following paragraphs, some additional information related to the investigation plan aiming to better define the masonry mechanical parameters and the results of structural dynamic identification are illustrated.

#### *3.1 Definition of Mechanical Properties of Masonry*

In situ and laboratory tests took place in order to determine (i) the constitution of mortars and stones (via chemical and mineralogical analyses) and (ii) the

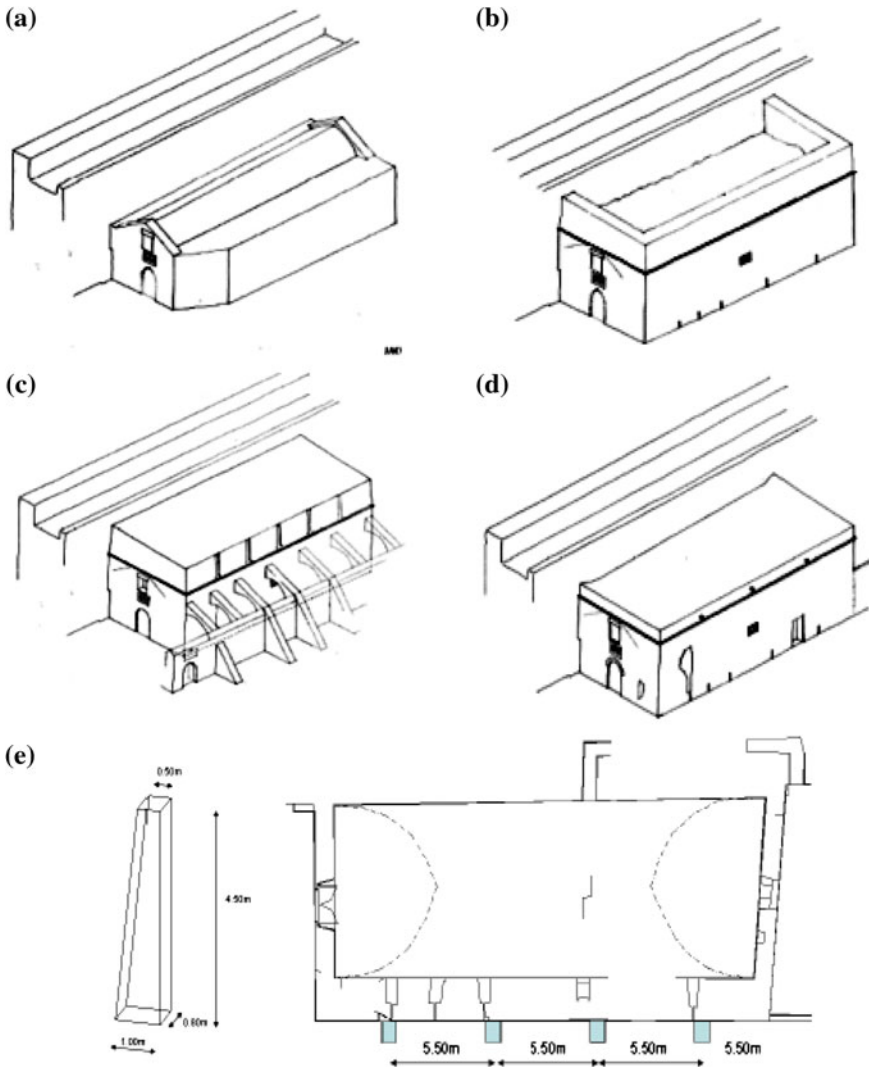


**Fig. 3** Constructive phases of the Arsenal de Milly, **a** the 1st phase during the G.M. De Milly era, **b** the 2nd phase during the G.M. Orsini era, **c** the 3rd phase during the Ottoman period and **d** the 4th phase during the Italian period, **e** the 5th and the contemporary phase after the restoration

compressive strength of these materials (via core borings). The results show that the mortars are pozzolanic-lime mortars and the stones are sand-limes.

More specifically, the pozzolanic-lime mortars have high content of fine aggregate (smooth surface, varying composition, natural origin) and its compressive strength varies from 3.14 to 4.56 MPa. The stones used are local sandstones (lime

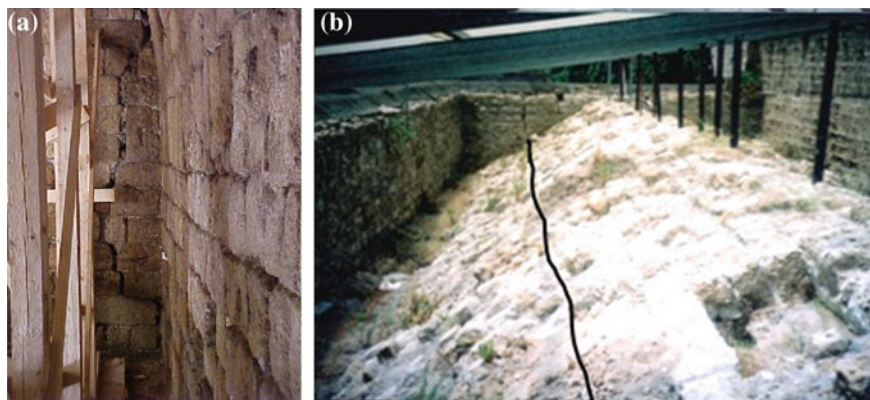


**Fig. 4** Pre-restoration damage pattern: detachment of the south wall (a) and longitudinal cracking on the vault (b)

**Table 1** Masonry properties

Compression strength $f_{wd}$	Shear limit strength $f_{vklim}$	Tension strength $f_{wt}$
1.8 MPa	0.2 MPa	0.18 MPa

stones) with compressive strength varying from 5.81 to 9.08 MPa and tensile strength at around 0.75 MPa.

Finally Table 1 shows the mechanical properties and the masonry's strength parameters to be adopted in the models. These values have been also adopted in a technical report, which concerns the restoration of the studied monument, conducted in the Aristotle University in Thessaloniki [31].

### ***3.2 Microtremor Measurements of the Structure Dynamic Characteristics***

The ambient vibration measurements have been performed to support the calibration of the models and of the mechanical parameters which rule the elastic phase [16]. The ambient vibration recording system used is based on a Guralp CMG-6TD three-component digital seismometer. The data acquisition system includes 8 sensors. The measurements were performed in two sets of at least 30 min long recordings. For each set, all utilized sensors were measuring simultaneously.

Figure 5 presents the location of the sensors in two different configurations. Figure 5a shows sensors 107, 109, 103 and 104 placed on the top of the structure while sensor 102 on the ground surface close to Arsenal De Milly: such configuration was addressed to identify the longitudinal mode of vibration. Figure 5b shows the sensors 107, 109, 108 and 104 placed in the four corners of the structure



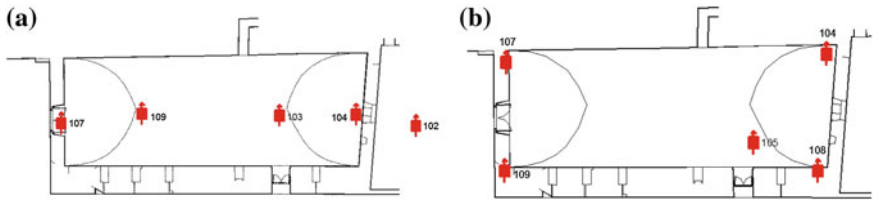


**Fig. 5** Sensors in the **a** longitudinal and **b** transversal direction

while the sensor 105 in an excavation inside the structure, this configuration mainly intended to identify the transversal mode of vibration.

For the longitudinal direction, Fig. 6a shows the Fourier spectral ratio given from the sensors situated on the corner near the defensive wall (107 and 104). On

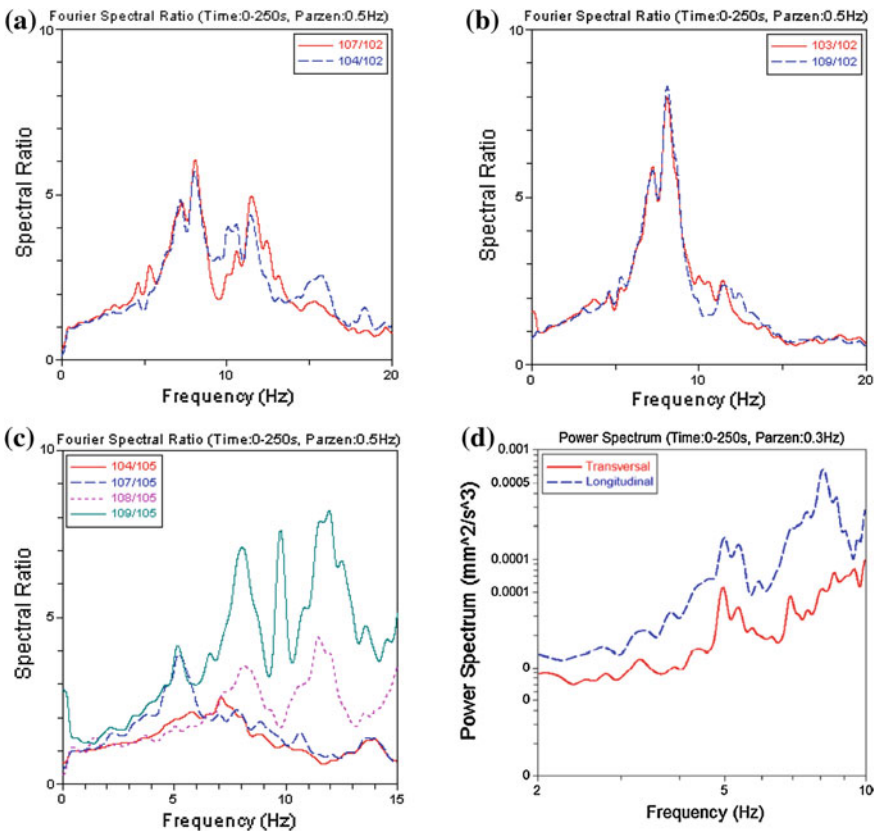


**Fig. 6** Fourier spectral ratio for the longitudinal direction—**a** sensors near the wall, **b** sensors near the center of the structure; **c** Fourier spectral ratio for the transversal direction; and **d** power spectrum from the FDD



this Fourier spectral ratio the first peak appears at the frequency of 8 Hz (0.125 s) while the second amplification appears at 11.6 Hz (0.086 s). Figure 6b shows the Fourier spectral ratio given from the sensors placed at the center of the vault (109 and 103). On this Fourier spectral ratio there is only one peak at the frequency of 8 Hz (0.125 s). These results verify that the structure is quite rigid in the longitudinal direction.

For the transversal direction, Fig. 6c shows the spectral ratio between the sensors placed in the four corners of the structure (107, 109, 108 and 104) and the sensor placed on the soil (105). Four frequencies are identified: 5.1 Hz (0.196 s), 8 Hz (0.125 s), 10 Hz (0.1 s) and 12 Hz (0.083 s). The sensor 109 placed in the south-east corner of the structure, presents for all the four frequencies more clear peaks and higher amplification compared to the other sensors (107, 108, 104). This may suggest an important torsional effect due to the different rigidity between the structure and the adjacent defensive wall and due to the opening (door) in one of the transversal walls.

Measurements were also analyzed by applying the Frequency Domain Decomposition (FDD) method (Fig. 6d) confirming the results discussed in the preceding; further details on this may be founded in [16].

## 4 Modeling

It is generally accepted that different modeling strategies may be adopted to analyze masonry structures. According to [4], models may be classified according to the following two criteria: scale of discretization (whether referring to the *material* phase or to the *structural element* level) and constitutive modeling of masonry (whether *continuous* or *discrete*). According to this classification, four model types can be identified: (1) Continuum Constitutive Law Models (CCLM), (2) Structural Element Models (SEM), (3) Discrete Interface Models (DIM), (4) Macro-Block Models (MBM). Models developed at the *material scale* are oriented to describe in an accurate way the complex behavior of masonry solids: at this scale, the composite nature of the material, which may be considered as heterogeneous (DIM) or homogenous (CCLM), plays a fundamental role. On the contrary, the driving idea of models developed at the *element scale* is to identify, within the masonry continuum, portions of structure subjected to recurrent damage modes (to this aim, post-earthquake damage observation is a remarkable source of information): the masonry structure is thus not seen as a “blurred” continuum but as a set of bodies with common mechanical behavior. Depending on the different classes of heritage buildings (churches, palaces, towers, defensive-walls) the choice of the most appropriate model for seismic assessment may vary.

In the examined case, the integrated use of different modeling strategies is proposed by adopting in particular: a CCLM model, developed using the OpenSees code [27] and adopting a Drucker-Prager yield criterion to simulate the masonry behavior; a SEM model, using the Tremuri software [21] that is based on the

equivalent frame approach; a MBM model, by using the MB-PERPETUATE software [20] based on limit analysis according to the kinematic approach.

This choice follows the discussion on the expected seismic behavior of the Arsenal de Milly illustrated in Sect. 1.

The CCLM global model allows to more accurately evaluate the combined in-plane and out-of-plane contribution to the global seismic response, in terms of both stiffness and strength. Indeed, the contribution associated with the out-of-plane response could be quite relevant in such a case due to the significant thickness of walls. This model is also adopted in order to calibrate the elastic mechanical parameters on the basis of measurements carried out from ambient vibration tests (see Sect. 4.3). It is also used to evaluate Soil-Foundation Interaction and flexible-foundation effects (see Sect. 5.4). Moreover it is particularly effective to evaluate the interaction effect with the massive adjacent defensive wall. Even though the quite simple configuration of the Arsenal de Milly does not pose huge difficulties in setting up such detailed models (their computational effort being often seen as unfeasible in the case of complex architectural configurations, at least at the global scale), the execution of nonlinear analyses up to very heavy damage states is difficult due to convergence problems. Indeed, this represents a crucial issue in particular in the context of PBA and masonry structures, which are characterized by a strong nonlinear behavior already from very low intensity levels of the seismic demand.

To overcome this limit and try out the reliability also of other modeling strategies, the SEM and MBM models have been adopted, too. Their use should be viewed jointly and in an integrated way. In fact, the SEM model, that neglects the out-of-plane contribution of walls, aims to evaluate the seismic response in the longitudinal direction (mainly owing to the in-plane response) and to account for the global interaction effects; whereas the MBM model is assumed as the most reliable strategy to evaluate the response of the arch system in the transversal direction. In the SEM model, the interaction effects with the massive defensive wall are simulated in an approximate way by considering different constraint configurations.

Finally, it is worth noting that the possible occurrence of local mechanisms in the massive defensive wall (for example, associated to the detachment of external leaves) has been neglected and the attention is only focused on the seismic response of the Arsenal de Milly.

In the following Sections, the utilized models for the seismic assessment are illustrated in detail, referring to the above mentioned categories (CCLM, SEM and MBM).

## ***4.1 CCLM Approach***

This model was developed using a continuum constitutive law for material properties. We assumed homogeneous material properties. The CCLM model is simulated using the finite element method and its geometrical and material properties

stem from the data obtained from the as-built information. Older studies, field measurements and laboratory surveys, as introduced in Sect. 3.1, were very helpful for the development of the final CCLM that was used herein.

Eight-node brick elements with 3 degrees of freedom at each node were used. The non-linear response is distributed to the whole structure by using Drucker-Prager plasticity law [10]. The Drucker-Prager yield criterion is defined in OpenSees code [27] by the following parameters: the bulk modulus  $k$  and the shear modulus  $G$  which are functions of the elastic modulus considered, the yield stress  $\sigma_Y$  and the frictional strength parameter  $\rho$ .

In order to calculate the values of the first two parameters ( $k$  and  $G$ ), the masonry’s elastic modulus  $E$  is taken equal to 900 MPa as calibrated on the basis of results from ambient vibration tests (see Sect. 4.3). The Drucker-Prager strength parameters, frictional strength parameter  $\rho$  and yield stress  $\sigma_Y$  could be related to the Mohr-Coulomb friction angle  $\phi$  and cohesive intercept  $c$  by evaluating the yield surfaces in a deviatoric plane as described by Chen and Saleeb [9]. This relation is based on the shear strength criterion as it is expressed in (1), where the shear strength with no compression is  $f_{vk0} = c = 0.2$  MPa, the frictional coefficient is  $\mu = \tan \phi = 0.4$  and  $\sigma_n$  is the compressive stress. The values used for the Drucker-Prager strength parameters are shown in Table 2. The mass density is equal to 22.4 kN/m<sup>3</sup> and the model is considered fixed at its base.

$$f_{vk} = f_{vk0} + \mu \cdot \sigma_n \tag{1}$$

Figure 7 illustrates some views of the CCLM model carried out with the OpenSees code; at this model the defensive wall is assumed to be monolithically connected to the rest of the structure.

### 4.2 SEM and MBM Approaches

In this case, the seismic analyses of the Arsenal de Milly have been performed using in an integrated way two different models: a SEM Model, by using the Tremuri software [21] based on the Equivalent Frame approach and a MBM model, adopted for the analysis of cross response of system vault-masonry walls by using the MB-Perpetuate software [20]. In particular, the MBM model analysis has been used in order to include in the assessment the effect of transversal response by including also the out-of-plane contribution of the walls. This was ignored in the global analysis (since one of the main hypothesis of the adopted SEM model is to consider only the in-plane response of walls). Out-of-plane response is considered

**Table 2** Parameters for Drucker-Prager plasticity law

Bulk modulus $k$	Shear modulus $G$	Yield stress $\sigma_y$	Frictional strength parameter $\rho$
500 MPa	300 MPa	0.12 MPa	0.272

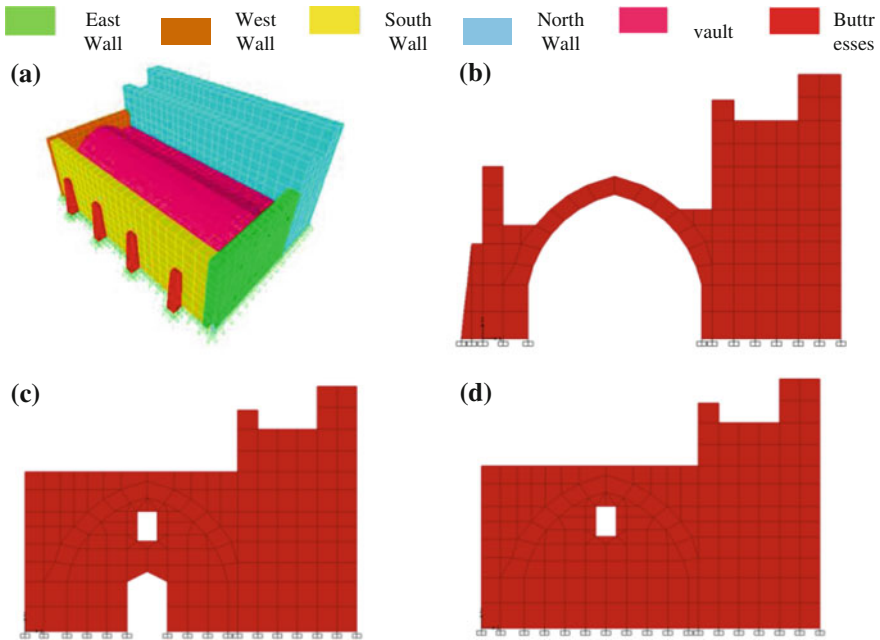


**Fig. 7** **a** 3D view of the spatial model with the 8 node brick elements (OpenSees), **b** 2D view of a typical cross section, **c** 2D view of the West Wall, **d** 2D view of the East Wall

very important for the examined case, due to its specific features (e.g. due to the presence of the buttr esses and the high thickness of walls).

According to the SEM model adopted, each wall is discretized by a set of masonry panels (piers and spandrels), in which the non-linear response is concentrated, connected by a rigid area (nodes). Thus starting from the 2D modeling of walls, the complete 3D model is obtained by introducing also floor elements: in particular, they are modeled as orthotropic membrane finite elements. For further detail, see also [22]. Figure 8 illustrates the structural model and the equivalent frame idealization of two transversal walls.

The analyses have been performed both in the X and in the Y directions. In the X direction, the effect of the interaction between the structure with the defensive wall has been modeled by considering the hypothesis of constrained horizontal displacements (Fig. 9). In the Y direction, no constraints are considered: in this direction, in fact, it has been assumed that the Arsenal de Milly is probably added in a second historical phase, so there is no adequate interconnection with the defensive walls; the analysis has been performed only in negative way by considering the constrain offered by the defensive wall in the other direction (Fig. 7).

The response of the panels was modeled by non-linear beams with a multilinear constitutive law that has been recently implemented in the Tremuri Program [5]. Figure 10 illustrates the force-deformation relationships assumed for masonry

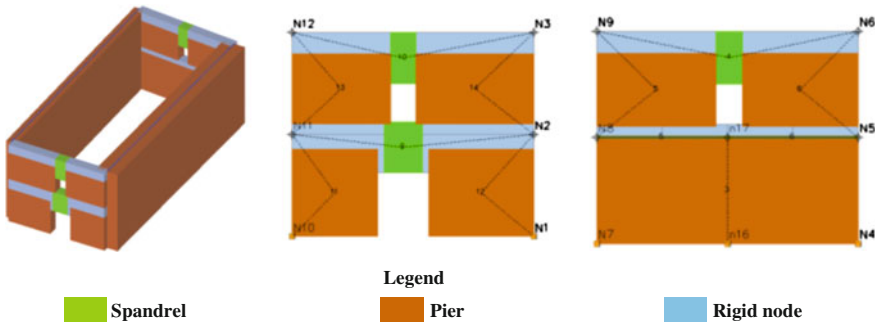


**Fig. 8** 3D view of the structural model (the visualization of the vault has been switch off) and equivalent frame model of two walls of the building

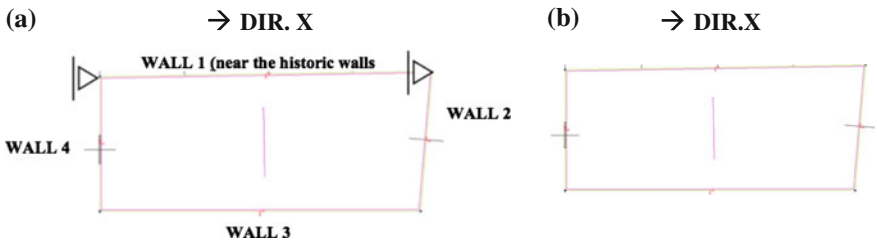
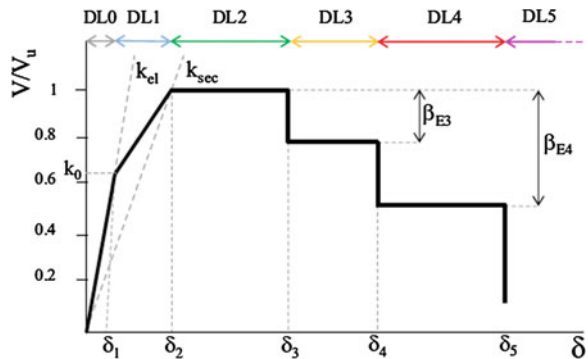


**Fig. 9** Constrains assumed in X direction in SEM model: with (a) or without (b) constrained horizontal displacements

**Fig. 10** Multi-linear constitutive laws for pier elements (where the legend of the damage levels DLs is illustrated in Fig. 17)



panels: it is based on a phenomenological approach that aims to describe the non-linear response of masonry panels until very severe damage levels (DL<sub>*i*</sub> with *i* = 1, ..., 5: DL<sub>1</sub>—slight, DL<sub>2</sub>—moderate, DL<sub>3</sub>—extensive, DL<sub>4</sub>—near collapse and DL<sub>5</sub>—complete collapse). Each DL is defined in terms of drift limits ( $\delta_E$ ) and corresponding strength decay ( $\delta_E$ ), defined for each of the basic failure modes

considered (e.g. Rocking, Diagonal Shear Cracking, Bed Joint Sliding or mixed one as well). Once DL5 is reached, the element contribution is only related to its capacity to support vertical loads. The initial elastic branch is directly determined by the flexural and shear stiffness of the panels. The maximum shear of the panel ( $V_u$ ) is computed according to some simplified criteria which are consistent with the most common ones proposed in the literature and codes (e.g. in Eurocode 8-3 [8]; ASCE SEI 41-06 [2] or the Italian Code for Structural Design 2008 [28]) and based on mechanical or phenomenological hypotheses by considering the occurrence of two possible failure modes (flexural or shear).

Table 3 illustrates the values of the mechanical parameters used in the analyses. The strength criterion used for piers and spandrels is according to [26] expressed by (2), with reference to the mortar failure domain:

$$\tau_u = \frac{c}{1 + \mu\phi_b} + \frac{\mu}{1 + \mu\phi_b} \sigma_y = \bar{c} + \bar{\mu}\sigma_y \tag{2}$$

where  $c$  and  $\mu$  are the local cohesion and the friction respectively (assumed equal to 0.2 and 0.6) and  $\phi_b$  is an interlocking parameter (assumed equal to 1) on basis of the texture and dimensions of ashlar masonry).

Floor elements—in this case the vault—are modeled in the Tremuri program as orthotropic membrane finite elements, in particular: normal stiffness provides a link between piers of a wall, influencing the axial force on spandrels ( $E_{1v}$ ); shear stiffness influences the horizontal force transferred among the walls ( $G_v$ ), both in linear and non-linear phases. In this case, the definition of the equivalent stiffness properties has been performed referring to the correlation laws proposed in [6] by considering the mechanical properties of masonry, adequately corrected through the use of specific coefficients aimed to establish an equivalence in terms of equivalent membrane and take into account the effect associated to the shape and geometrical proportion of the vault (e.g. rise-to-span ratio). As described in [6], such coefficients have been obtained by the elastic numerical simulation of various vault (barrel, cross and cloister) response, in case of pre-defined load configurations aimed to schematize an axial-only and pure shear behaviour as illustrated in Fig. 11.

In particular, based on the geometrical features of the examined vault, that are similar to a barrel vault, a value of the rise-to-span ratio approximately equal to 0.3 has been assumed, leading to a ratio of  $E_{2v}/E$  and  $G_v/G$  equal to 0.3 and 0.55, respectively; moreover, the ratio  $E_{1v}/E$  has been assumed equal to 1.6. Figure 11 illustrates the results related to the  $G_v/G$  ratio for different vault configurations.

**Table 3** Mechanical parameters associated with masonry panels (piers and spandrels) and the vault

Mechanical properties	
Masonry panels	Diaphragms
$E = 900 \text{ MPa}$	$E_{1v} = 270 \text{ MPa}$
$G = 300 \text{ MPa}$	$E_{2v} = 1440 \text{ MPa}$
$\bar{c} = 0.125$	$G_v = 165$
$\bar{\mu} = 0.375$	$t = 0.85 \text{ m}$

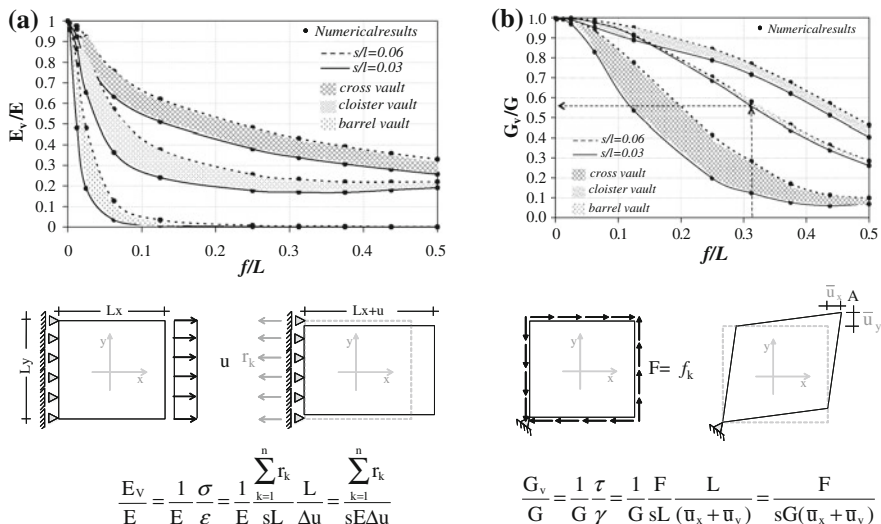


**Fig. 11** Ratio  $E_v/E$  (a) and  $G_v/G$  (b) by varying different types of structural vaults [6] and corresponding boundary conditions assumed to simulate the condition of pure-axial and shear state on vaults and establish the equivalence with the equivalent membrane

The analysis of the cross response has been performed by using the MB-Perpetuate software [20], developed in the framework of the PERPETUATE Project. Figure 12 illustrates the analyzed model (the initial configuration and the deformed one), where the plastic hinges are indicated with a grey circle. Their position has been defined on the basis of the expected response, evaluated from the observation of the recurrent seismic damage of vaulted structures and by taking into account the specific condition of constrains which characterized the examined case. In the case of the hinge located at the base of the pillar on the left, two hypotheses have been

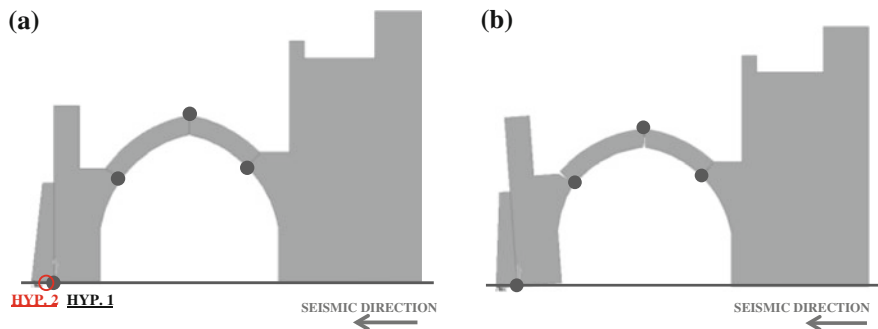


**Fig. 12** MBM model: **a** identification of the collapse mechanism and position of hinges; **b** deformed configuration



considered as a function of the contribution offered by the buttress to the stability against overturning. This is related to the quality of interlocking secured between the buttress and the masonry wall: whether completely effective (Hyp.2) or not (Hyp.1).

### 4.3 Calibration of Elastic Parameters of the CCLM Model

In order to calibrate the elastic behavior of the model in OpenSees, the modal analysis results in terms of period values are compared with the values obtained by ambient vibration measurements.

To this aim, parametric analyses have been performed with different assumptions on the Young Modulus  $E$  (if representative of cracked or un-cracked conditions and also by differentiating the values adopted for the main body and the defensive wall), but under the conventional hypothesis of a fixed restraint at the foundation.

As indicated in Table 4, the best match with the experimental results is obtained if an elastic modulus equal to 900 MPa is assumed for both the main structure and the fortified wall. This value agrees with the effective elastic modulus value, which is reduced by 50 % compared to the initial value that resulted from experimental measurements ( $E_{\text{initial}} = 1800$  MPa). The 50 % reduction is consistent with the values proposed in the Italian Code for Structural Design 2008 [28] and in Eurocode 8 [8].

Of course, other uncertainties could also affect this calibration, such as the role played by the soil-foundation-structure interaction. This issue is briefly discussed in Sect. 5.4, while the complete PBA of the asset is performed in the following by considering for all models the hypothesis of a fixed base condition.

The first and the fourth modes of the model (OpenSees) are the most significant as a high mass percentage is activated. In the first mode the predominant displacements are in the transversal direction (Table 5) and the period ( $T_1$ ) is equal to 0.198 s. The second and the third modes activate a negligible mass fraction (Table 5). In the fourth mode the predominant displacements are in the longitudinal direction (Table 5) and the period ( $T_4$ ) is equal to 0.126 s. As evident from Table 4, the first and fourth periods fit quite well the experimental results. The mode shapes for the global model in OpenSees are illustrated in Fig. 13 whereas their mass participation factor is listed in Table 5.

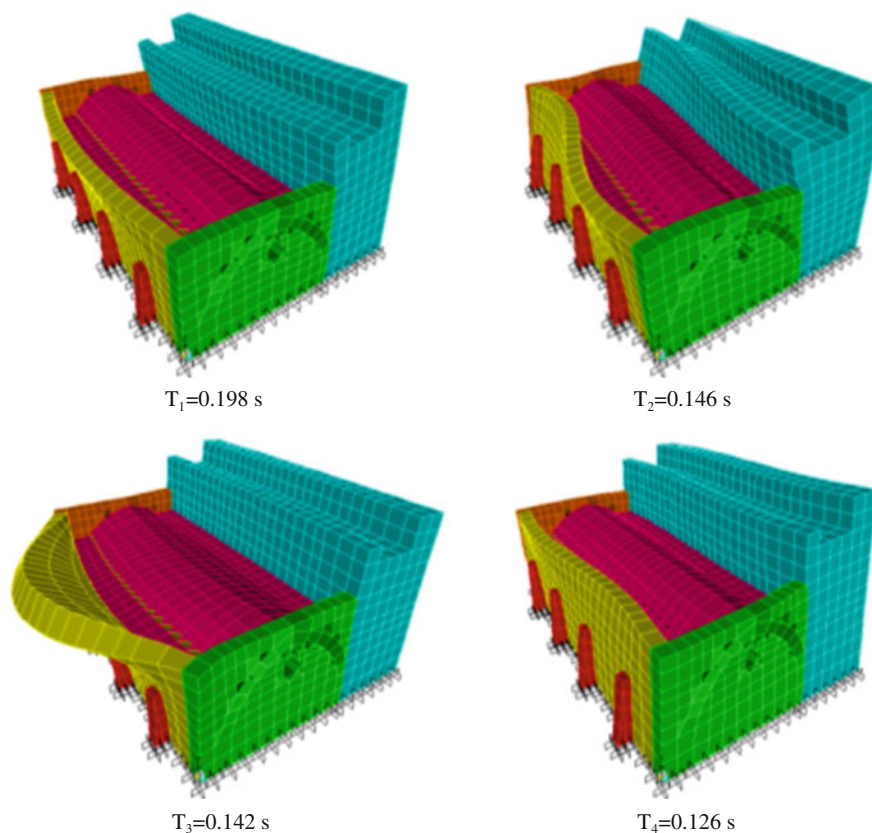
Moreover, concerning the rotational modes of vibration, it was found that they are important and activate a high percentage of total mass in the 1st, 2nd and 4th modes.

**Table 4** Comparison of the fundamental periods in the two directions as resulted from OpenSees and from microtremor measurements

	Global model (OpenSees)	Ambient vibration measurements
$T_1$ (s)	0.198	0.196
$T_4$ (s)	0.126	0.125

**Table 5** Modal participating mass ratios for the all the degrees of freedom, translational ( $U_x$ ,  $U_y$ ,  $U_z$ ) and rotational ( $R_x$ ,  $R_y$ ,  $R_z$ )

Mode	$U_x$ (%)	$U_y$ (%)	$U_z$ (%)	$R_x$ (%)	$R_y$ (%)	$R_z$ (%)
1	<b>60.70</b>	0.00	0.04	0.02	<b>23.65</b>	<b>26.97</b>
2	0.01	0.03	0.00	0.00	0.02	<b>11.74</b>
3	1.06	0.00	0.13	0.08	0.09	0.34
4	0.00	<b>68.49</b>	0.00	<b>22.99</b>	0.00	<b>30.89</b>

**Fig. 13** Mode-shapes and the period values obtained by OpenSees for Arsenal de Milly in the 3D model

Once the parameters of the numerical model are established in order to have the same periods of vibration for the modal analysis and the experimental data, dynamic analysis was performed with the model. The input for the dynamic analysis is scaled to have a very small value of amplitude ( $0.4 \text{ m/s}^2$ ) in order to avoid structural damage. The numerical output of this analysis for different nodes on the top of the structure was collected and was subsequently used as input in ARTeMIS program [1].

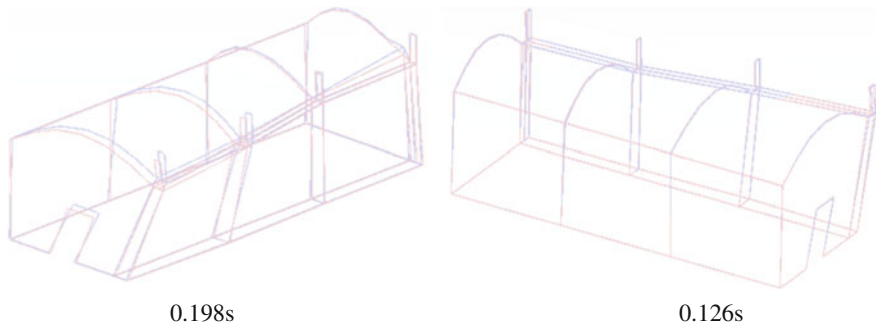


**Fig. 14** Comparison of the FDD derived mode shapes from ambient vibration (*red*) and from OpenSees outputs (*blue*) for two periods: 0.198 and 0.126 s

This step allows detecting the shape modes that come from numerical dynamic analysis. All modes are identified using the Frequency Domain Decomposition (FDD) technique. Several modes in the frequency range of 1–25 Hz could be identified, but only four modes (Table 5) are reasonably unchanged considering different data sets and seem stable. Figure 14 shows the comparison between the mode shapes (for the periods 0.198 and 0.126 s) computed using the experimental data (red lines) and numerical data obtained from the outputs of the dynamic analysis performed with OpenSees (blue lines). Modal Assurance Criterion (MAC) which is employed to quantify the differences between two mode shapes is equal to 0.986 s for the period of 0.126 and 0.768 s for the period of 0.198 s.

## 5 Seismic Assessment

### 5.1 Seismic Hazard

In this paragraph the seismic hazard assumed for the PBA of Arsenal de Milly is presented. According to the results of past geophysical surveys and field measurements that were conducted in the Medieval city of Rhodes, the studied monument could be classified in soil class C according to EC8 soil classification scheme [7]. Due to the quite rigid and massive response of the structure, the Peak Ground Acceleration (PGA) has been assumed as appropriate Intensity Measure (IM) to define the seismic demand. A vector-valued probabilistic seismic hazard assessment (VPSHA) methodology was used for the estimation of a uniform hazard spectrum for Arsenal de Milly of Rhodes for three return periods [14]. The hazard curve, presented in Fig. 15b, shows the annual frequency of exceedance ( $\lambda_R$ ) as a function of the peak ground acceleration PGA: in particular the value corresponding to the return period of the performance level considered for the PBA ( $\bar{T}_{3B} = 475$  years) is equal to  $1.78 \text{ m/s}^2$ . Figure 15a shows the elastic displacement-acceleration response spectra (ADRS format) assumed for performing the PBA in the case of nonlinear static analyses.

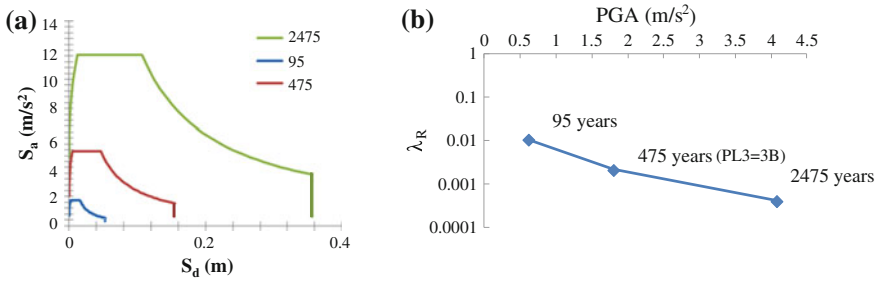


**Fig. 15** a Seismic demand in ADRS format according to EC8 (soil class C) for three return periods (95, 475 and 2475 years); b hazard curve (from Gherboudj et al. [14])

### 5.2 Results of Nonlinear Static Analyses and Definition of Performance Levels

Figure 16 illustrates the results of the comparison, in terms of pushover curves, between the different modeling strategies discussed in the preceding. These curves have been obtained by performing nonlinear static analyses in both seismic directions, in the case of CCLM and SEM models, and a nonlinear kinematic analysis, in the case of MBM model. Furthermore, in the case of the SEM models the legend “with constraints” and “no constraints” refers to the boundary conditions explained in Fig. 9. In the SEM models pushover analyses have been performed by adopting a load pattern proportional to masses (with forces applied only in nodes) and by increasing the displacement of a node located in wall 3 (see Fig. 9). In the case of the CCLM, to simulate a load pattern proportional to masses, the nonlinear static analysis has been performed by applying a horizontal force to each node, which results from the mass of this node multiplied to the gravity acceleration; this load pattern increases gradually until the collapse of the building [29]. Due to the more dense mesh of CCLM model than that of SEM one, the first guarantees a more distributed load. The application of lumped masses only in few nodes is usual in the case of the equivalent frame idealization; of course, in the case of massive structure, this hypothesis can be more conventional. In this case, the adoption of more models, allows also to verify the effects of such approximations and uncertainties.

In the case of MBM, the curve describes the progressive development of the collapse multiplier  $\alpha$  (that induces loss of equilibrium of the system) for increasing finite values of the generalized displacement  $d$ , up to the value for which  $\alpha(d) = 0$ . In particular, as proposed in [18] a bilinear curve with an initial pseudo-elastic period has been considered: this latter has been assumed equal to that coming from the first modal shape in Y direction as discussed at Sect. 4.3.

In case of the CCLM, it is worth noting that the base shear has been computed by considering only the contribution provided by nodes on masonry walls of the main body of Arsenal de Milly by neglecting that of the defensive wall (that is quite significant due to the huge thickness); the same in the case of Tremuri program, too.

Despite this, the global model allows to account for the mutual interaction effects. Regarding the analyses in OpenSees, it is important to note that it has been possible to reach convergence just until the part of the curve drawn with a continuous line, and then only a suitable trend has been traced (illustrated with the dashed line in Fig. 16). Pushover curves of SEM and CCLM models are comparable. In general, the base shear resulting from the CCLM model is higher than the one obtained by the SEM model. Furthermore, it has to be noted that, with reference to the transversal direction, the initial stiffness obtained with the CCLM model is higher: this effect could be associated with interaction between the structure and the defensive wall.

On each curve, four Damage Levels (DLs)—assumed coincident with the corresponding PL are marked in red; the third one corresponds to 3B performance level considered for the PBA. They have been obtained by applying the multi-scale approach proposed in [19], in the case of nonlinear static analyses, and following the criteria proposed in [18], in the case of the nonlinear kinematic analyses.

According to the multi-scale approach, the definition of DLs takes into account the asset response at different scales: local damage (structural elements scale, E), architectural elements scale (damage in macroelements M, like as masonry walls or diaphragms) and global scale (G, pushover curve). To this aim, proper variables are introduced at each scale to monitor the progress of nonlinear response. Since the

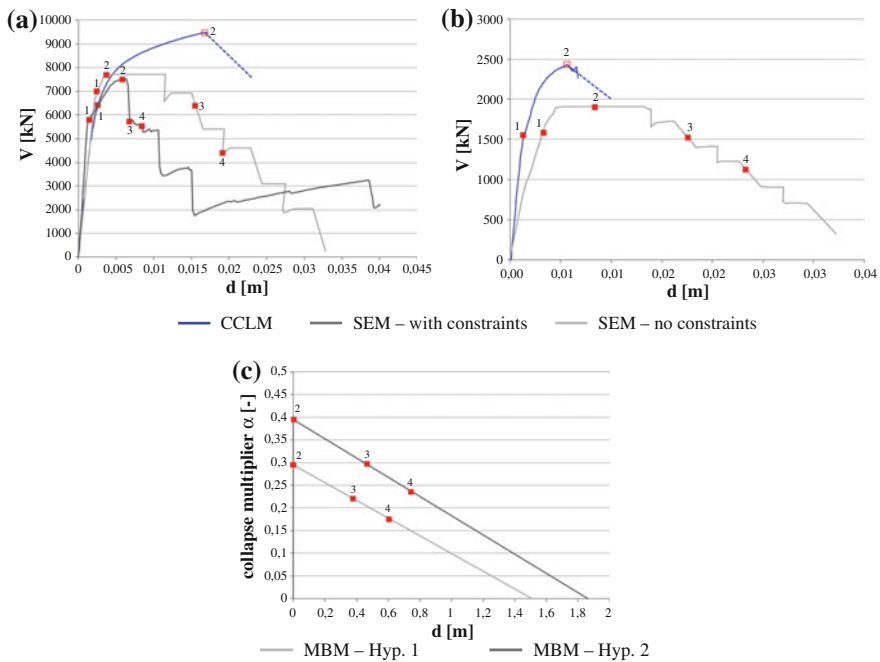


**Fig. 16** Comparison between pushover curves obtained by using: SEM and CCLM models in **a** X direction and in **b** Y direction; **c** collapse multiplier for MBM model in Y direction

final seismic assessment is made through the global pushover curve, the displacement corresponding to attaining DLk ( $k = 1, \dots, 4$ ) is then computed as:

$$d_{DLk} = \min(d_{E,DLk}; d_{M,DLk}; d_{G,DLk}) \quad k = 1, \dots, 4 \tag{3}$$

where  $u_{E,DLk}$ ,  $u_{M,DLk}$ , and  $u_{G,DLk}$  are the displacements on the pushover curve corresponding to the attainment of predefined limit conditions at the aforementioned scales, respectively.

In the examined case the following variables have been monitored: drift  $\delta_E$  (at element scale); interstorey drift  $\theta_{w,l}$  (being  $w$  the wall number and  $l$  the level considered) and percentage of residual strength on the pushover curve of each single wall  $\kappa_M$  (at macroelement scale); percentage of residual strength on the overall pushover curve  $\kappa_G$  (at a global scale). The limit thresholds assumed for these variables are summarized in Table 6. The application of the multi-scale approach has been extended to more complex cases by introducing additional checks as in [19].

In the case of MBM model, the displacement capacities corresponding to the attainment of DL3 and DL4 are defined as  $0.25d_0$  and  $0.4d_0$ , respectively (where  $d_0$  is the displacement corresponding to zero residual strength in the capacity curve); such limits have been calibrated on the basis of nonlinear dynamic analyses [18].

Figure 17 illustrates the damage pattern at DL3 of the most significant walls (defined in Fig. 9), as obtained by the nonlinear static analyses performed in Tremuri. As it is possible to deduce by the damage pattern, in the X direction the presence of the constrains induces a torsional effect, so that the orthogonal walls

**Table 6** Variables and limit thresholds assumed at the three scales considered for the multiscale approach, which was applied in the case of the SEM model

Scale	Variable	Threshold assumed for the attainment of the corresponding DLk at global scale (%)			
		DL1	DL2	DL3	DL4
Local—piers	$\delta_E^a$	–	0.3/0.6	0.5/1	0.7/1.5
			(70/100)	(30/85)	(0)
Local—spandrels	$\delta_E^b$	0.3(50)	0.6(50)	2(0)	–
Macroelement	$\theta_{w,l}$	0.1	0.3	0.5	0.7
	$\kappa_M$	–	100	70	40
Global	$\kappa_G$	$\geq 50$	100	80	60

*Notes*

<sup>a</sup>The two values refer to the limits assumed for the shear and flexural failure mode, respectively. According to the multilinear constitutive laws assumed, progressive strength decay corresponds to the attainment of such drift thresholds. In particular, values summarized in brackets refer to the corresponding residual strength assumed. In the case of piers, the attainment of a DLk at a global scale is monitored by checking for the DLi attainment with  $i = k + 1$

<sup>b</sup>The meaning of terms is the same for piers. In the case of spandrels, no distinction is made with regards to the failure mode, but values have been adopted taking into account the architrave type (arch system). In the case of spandrels, reaching a DLk at the global scale is monitored by checking for the DLi attainment with  $i = k + 2$

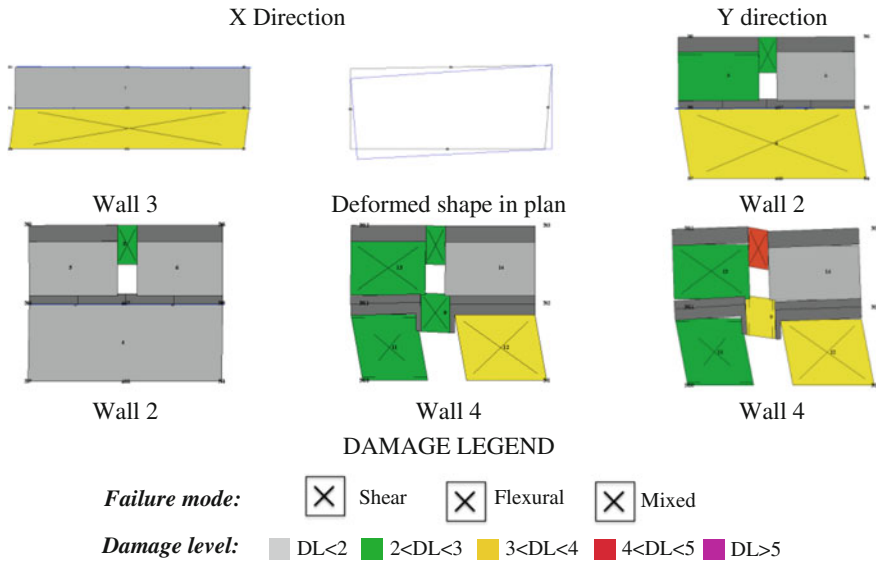


**Fig. 17** SEM model: damage pattern at DL3 of the most significant walls (in the case of X direction the damage patterns refer to the model with horizontal constraints)

(walls 2 and 4) are mainly involved, while in the longitudinal walls only wall 3 is subjected to the seismic action: in fact, the horizontal loads toward this direction in the wall 1 are applied directly to the constrains. In Y direction, unlike the walls 1 and 3, the walls 2 and 4 are involved, developing a quite relevant damage pattern, due to the fact that they are directed toward the seismic action.

### 5.3 Safety Verification

Figure 18 shows the comparison of the results from all the models used in terms of the maximum Intensity Measure selected ( $IM = PGA$ ) compatible with the fulfillment of performance levels that have to be checked ( $IM_{3B}$ ). For completeness the IM values associated with the attainment of DL2 and the corresponding return periods (as derived from the hazard curve shown in Fig. 15b) are illustrated. In the case of the CCLM model only the values corresponding to DL2 have been computed, due to the numerical difficulties in evaluating the softening phase of the pushover curve: the case namely as “CCLM-I” refers to the result obtained by considering in the evaluation of the capacity curve also the contribution of the defensive wall (obviously in terms of both base shear and mass, thus seismic action). The value of the seismic demand (in terms of PGA and return period) at PL3 is marked in Fig. 18 with a red line.



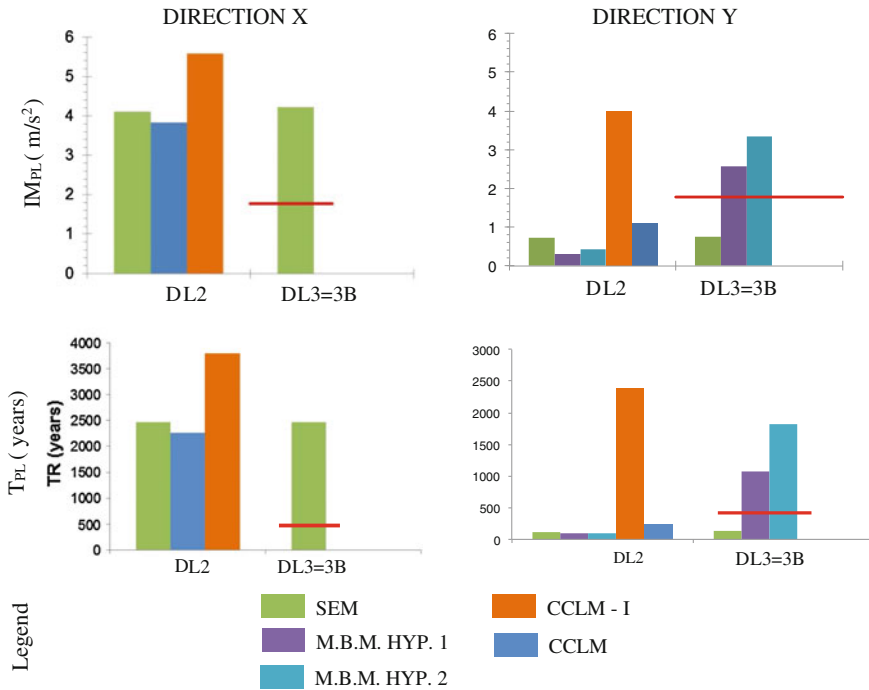


**Fig. 18** Comparison between maximum acceleration and return period at PL2 and PL3 in the models used

Such values have been computed according to the procedure illustrated in [19], mainly based on the Capacity Spectrum Method [12] and the use of over-damped spectra. The conversion of the pushover curve into Equivalent Degree of Freedom has been performed by using the  $\Gamma$  and  $m^*$  factors (by assuming an eigenvector coming from the modal analysis and the participation mass) as proposed by Fajfar [11] and assumed also in Eurocode 8 [7]. The overdamped spectra have been computed by assuming the reduction factor proposed in Eurocode 8, by computing the equivalent damping of the structure ( $\xi_{equ}$ ) from the following expression [3]:

$$\xi_{equ} = \xi_{el} + \alpha \left( 1 - \frac{1}{\mu^\beta} \right) \tag{4}$$

where:  $\xi_{el}$  is the elastic damping assumed equal to 5 %;  $\alpha$  and  $\beta$  have been assumed equal to 20 and 1, respectively; and  $\mu$  is the ductility value.

Regarding the results in Y direction (where the prevalent structure seismic response is the out-of-plane one), the more reliable model is the MBM: these results are on the safe side with respect to those of CCLM model, while the seismic assessment obtained by using the SEM model is considered completely conventional (since the out-of-plane contribution is neglected in this latter model). In X

direction, where the in-plane response is predominant, the SEM model seems to adequately describe the seismic behavior of the structure in comparison with the more refined CCLM model. In general, all the analyses determine results more conservative than the values obtained by the CCLM model.

In terms of outcome of the PBA, the seismic verification at PL3 is satisfied referring to the MBM model for the Y direction and referring to the other models for the X direction.

#### ***5.4 Analysis of the Soil-Foundation Interaction Effects***

Pitilakis and Karatzetzou in their study [30] proposed a methodology for the assessment of earthquake response of monuments with flexible masonry foundation, considering soil-foundation interaction. In this study, finite stiffness representing flexible masonry foundations (surface and embedded) is provided for horizontal, vertical and rocking modes of vibration with respect to the foundation, wall-to-soil elasticity moduli ratios  $E_w/E_s$ , for certain  $h/b$  ratios ( $h$  is the total height of the foundation and  $b$  is the half-width of the foundation). Foundation type and geometry were carefully chosen from existing monuments extracted from the database of the PERPETUATE project ([www.perpetuate.eu](http://www.perpetuate.eu), [24]). Representative rectangular foundations of varying dimensions were chosen for the analyses. The main steps of the proposed methodology are the following:

- (i) evaluation of the dimensionless frequency  $\alpha_0$ , ( $\alpha_0 = \omega r/V_s$ , where  $\omega$  = cyclic excitation frequency,  $r$  = characteristic foundation dimension and  $V_s$  = shear wave velocity of soil profile) which should not exceed the value of 1. When the dimensionless frequency  $\alpha_0$  is lower than unity, the dynamic stiffness of a foundation section can be approximated adequately by the “static stiffness”, the latter being the stiffness of the foundation-soil system under small-strain (static) loading [15];
- (ii) calculation of “static” stiffness  $K_{\text{static}}$  of the foundation—soil system, for all translational and rotational modes from analytical solutions proposed in literature for rigid foundations [13];
- (iii) calculation of the  $E_w/E_s$  ratio and finally
- (iv) evaluation of the reduction of stiffness of the flexible masonry wall foundation compared to the rigid one by the proposed diagrams.

The above-mentioned formula has been utilized for the investigation of the effects of soil—foundation—structure—interaction on Arsenal De Milly [30] as well as on other monumental structures (e.g. in [17]). Modal and pushover analyses were performed for two models with the following assumptions for the base restraints: (i) fully fixed condition (as already discussed in the previous sections); and (ii) with appropriate impedances at the centroid of the foundation. Herein only the main results in terms of percent period lengthening due to SFSI and foundation flexibility (from a modal analysis) and pushover curves (from a nonlinear static

**Table 7** Percent modification of the structure period for the first 5 modes of vibration

	(SFSI-fixed)/fixed (%)
Mode 1	6.30
Mode 2	7.60
Mode 3	5.0
Mode 4	17.0
Mode 5	7.70

*FIXED* Fixed-base structure and *SFSI* The actual structure founded on a flexible wall foundation

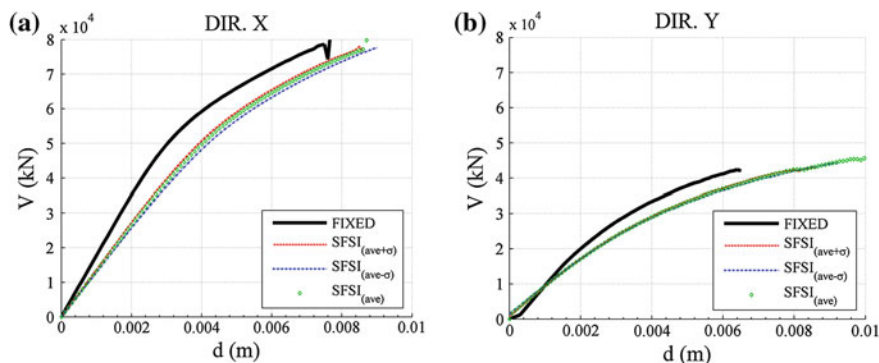


**Fig. 19** Pushover curves in two directions (a) X direction and (b) Y direction for the examined models

analyses) are presented, whereas in [30] a more comprehensive description is provided. Table 7 shows the percent modification of the structure period (period lengthening from 5 % up to 17 %) due to SFSI and foundation flexibility effects, for the first five modes of vibration, while Fig. 19 depicts the pushover curves of the two examined models. From the results it is surmised that foundation flexibility and soil-foundation interaction inevitably increase the compliance of the system. The pushover curves in Fig. 19 show that the maximum strength of both fixed- and flexible-base models is approximately equal. The maximum displacement, however, and, consequently, the ductility of the flexible-base model are considerably increased compared to the fixed-base one, especially in the transversal (Y) direction, i.e. along the flexible side of the structure, where the out-of-plane response is predominant.

## 6 Conclusions

This chapter presented results from seismic assessment of the Arsenal de Milly according with the procedures proposed in the PERPETUATE project, with particular emphasis placed on results provided by different modeling strategies.

Although the structure is quite simple from a geometrical point of view, its seismic response is quite interesting due to the interaction effects with the massive adjacent defensive wall. Calibration of models was supported by the results of ambient vibration tests that are very useful in such case in order to highlight torsional modes related to the mentioned interaction effects. Seismic assessment results proved that the structure is able to fulfill a seismic demand associated with a return period of 475 years. In particular, the MBM (for the transversal direction) and CCLM and SEM models (for the longitudinal direction) seem the more adequate modeling strategies for a reliable assessment. Although the CCLM model is more refined than the SEM one, in nonlinear range it experienced some numerical/convergence problems: thus, the combined use of the SEM model is useful to corroborate the results achieved and allow to perform the analyses until a strong nonlinear range. Soil—foundation—structure interaction and foundation flexibility seems to affect the results and should be considered in the analyses. In the present study, even if the entire PERPETUATE procedure considering such effects has not been applied, the comparison between the pushover curves obtained by considering or neglecting these effects allowed to highlight the main differences in response.

## References

1. ARTeMIS (2009) ARTeMIS Extractor pro 2009. s.l. Denmark, SVIBS. <http://www.svibs.com/>
2. ASCE/SEI 41-06 (2007) Seismic rehabilitation of existing buildings. American Society of Civil Engineers, Reston, VA
3. Blandon CA, Priestley MJN (2005) Equivalent viscous damping equations for direct displacement based design. *J Earthq Eng* 9(Special Issue 2):257–278
4. Calderini C, Cattari S, Lagomarsino S, Rossi M (2010) Review of existing models for global response and local mechanisms. PERPETUATE (EU-FP7 Research Project), Deliverable D7 ([www.perpetuate.eu/D7/](http://www.perpetuate.eu/D7/))
5. Calderini C, Cattari S, Degli Abbatì S, Lagomarsino S, Ottonelli D, Rossi M (2012) Modelling strategies for seismic global response of building and local mechanisms. PERPETUATE (EU-FP7 Research Project), Deliverable D26. [www.perpetuate.eu/D26/](http://www.perpetuate.eu/D26/)
6. Cattari S, Resemini S, Lagomarsino S (2008) Modelling of vaults as equivalent diaphragms in 3D seismic analysis of masonry buildings. In: Proceedings 6th international conference on structural analysis of historical construction, Bath, UK
7. CEN (European Committee for Standardization) (2004) Eurocode 8: design of structures for earthquake resistance, Part 1: General rules, seismic actions and rules for buildings. EN1998-1:2004. Brussels, Belgium
8. CEN (European Committee for Standardization) (2005) Eurocode 8: design of structures for earthquake resistance, Part 3: Assessment and retrofitting of buildings. EN 1998-3:2005. Brussels, Belgium
9. Chen WF, Saleeb AF (1994) Constitutive equations for engineering materials. In: *Elasticity and modelling*, vol. I. Elsevier, New York
10. Drucker DC, Prager W (1952) Soil mechanics and plastic analysis for limit design. *Q Appl Math* 10(2):157–165

11. Fajfar P (2000) A non linear analysis method for performance-based seismic design. *Earthq Spectra* 16(3):573–592
12. Freeman SA (1998) The capacity spectrum method as a tool for seismic design. In: *Proceedings 11th European conference of earthquake engineering*, Paris, France
13. Gazetas G (1991) Formulas and charts for impedances of surface and embedded foundations. *J Geotech Eng* 117(9):1363–138
14. Gherboudj F, Laouami N, Benour D (2011) Report on vector-valued characterization of seismic hazard with respect to strong-motion parameters, PERPETUATE (EU-FP7 Research Project), Deliverable D24. [www.perpetuate.eu/D24/](http://www.perpetuate.eu/D24/)
15. Iguchi M, Luco JE (1981) Dynamic response of flexible rectangular foundations on an elastic half-space. *Earthq Eng Struct Dyn* 9:239–249
16. Karatzetzou A, Negulescu C, Manakou M, François B, Seyedi D, Ptilakis D, Ptilakis K (2015) Ambient vibration measurements on monuments in the Medieval City of Rhodes, Greece. *Bull Earthq Eng* 13(1):331–345. doi:[10.1007/s10518-014-9649-2](https://doi.org/10.1007/s10518-014-9649-2)
17. Karatzetzou A, Ptilakis D, Kržan M, Bosiljkov V (2015) Soil–foundation–structure interaction and vulnerability assessment of the Neoclassical School in Rhodes, Greece. *Bull Earthq Eng* 13(1):411–428. doi:[10.1007/s10518-014-9637-6](https://doi.org/10.1007/s10518-014-9637-6)
18. Lagomarsino S (2015) Seismic assessment of rocking masonry structures. *Bull Earthq Eng* 13(1):97–128. doi:[10.1007/s10518-014-9609-x](https://doi.org/10.1007/s10518-014-9609-x)
19. Lagomarsino S, Cattari S (2015) PERPETUATE guidelines for seismic performance-based assessment of cultural heritage masonry structures. *Bull Earthq Eng* 13(1):13–47. doi:[10.1007/s10518-014-9674-1](https://doi.org/10.1007/s10518-014-9674-1)
20. Lagomarsino S, Ottonelli D (2012) A Macro-Block program for the seismic assessment (MB-PERPETUATE), PERPETUATE (EU-FP7 Research Project), Deliverable D29. [www.perpetuate.eu/final-results/reports/](http://www.perpetuate.eu/final-results/reports/)
21. Lagomarsino S, Penna A, Galasco A, Cattari S (2012) TREMURI program: seismic analyses of 3D masonry buildings, University of Genoa (mailto:tremuri@gmail.com)
22. Lagomarsino S, Penna A, Galasco A, Cattari S (2013) TREMURI program: an equivalent frame model for the nonlinear seismic analysis of masonry buildings. *Eng Struct* 56:1787–1799. <http://dx.doi.org/10.1016/j.engstruct.2013.08.002>
23. Lagomarsino S, Abbas N, Calderini C, Cattari S, Rossi M, Ginanni Corradini R, Marghella G, Mattolin F, Piovanello V (2011) Classification of cultural heritage assets and seismic damage variables for the identification of performance levels. In: *Proceedings 12th international conference on structural studies, repairs and maintenance of heritage architecture (STREMAH)*, 5–7 Sept 2011, ChiancianTerme (Italy), WIT Trans Built Environ, vol 118, pp 697–708. doi:[10.2495/STR110581](https://doi.org/10.2495/STR110581)
24. Lagomarsino S, Modarelli H, Ptilakis K, Bosiljkov V, Calderini C, D’Ayala D, Benour D, Cattari S (2010) PERPETUATE project: the proposal of a performance-based approach to earthquake protection of cultural heritage. *Adv Mater Res* 133–134:1119–1124. *Trans Tech Publications*, Switzerland
25. Mamaloukos et al (1997) Survey of the Arsenal De Milly at the NE corner of the Fortification Wall of Rhodes
26. Mann W, Müller H (1980) Failure of shear-stressed masonry—an enlarged theory, tests and application to shear-walls. In: *Proceedings international symposium on load-bearing Brickwork*, London, UK, pp 1–13
27. McKenna F, Fenves GL, Jeremic B, Scott MH (2007) Open system for earthquake engineering simulation. <http://opensees.berkeley.edu/>
28. NTC 2008 Decreto Ministeriale 14/1/2008 (2008) Norme Tecniche per le costruzioni. Ministry of Infrastructures and Transportations. G.U. S.O. n. 30 on 4/2/2008 (in Italian)

29. Pantazopoulou SJ (2013) State of the art report for the analysis methods for unreinforced Masonry heritage structures and monuments. Research report. <http://ecpfe.oasp.gr/en/node/89>
30. Ptilakis K, Karatzetzou A (2014) Dynamic stiffness of monumental flexible masonry foundations. *Bull Earthq Eng.* doi:[10.1007/s10518-014-9611-3](https://doi.org/10.1007/s10518-014-9611-3)
31. Ptilakis K, Galazoula J, Sextos A (2002) Stability issues of the foundation of the fortification of the medieval city of Rhodes—Arsenal De Milly: pathology, static and earthquake resistance study of rehabilitation and restoration. Technical report (in Greek), Laboratory of Soil Mechanics, Foundation & Geotechnical Earthquake Engineering, Civil Engineering Department, Aristotle University of Thessaloniki